THE EFFECT OF TOPOGRAPHY ON THE IMPACT CRATERING PROCESS ON LUTETIA.

D. Elbeshausen[1], K. Wünnemann[1], H. Sierks[2], J. B. Vincent[2], and N. Oklay[2], [1]Museum für Naturkunde, Leibniz Institute for Research on Evolution and Biodiversity, Invalidenstr. 43, D-10115 Berlin, Germany, [2]Max-Planck-Institut für Sonnensystemforschung, Max-Planck-Straße 2, D-37191 Katlenburg-Lindau, Germany
Contact: dirk.elbeshausen@mfn-berlin.de; http://www.iSALE-code.de

Introduction: On 10 July 2010 the Rosetta spacecraft approached the main belt asteroid 21 Lutetia at a distance of 3170 km. The Optical, Spectroscopic, and Infrared Remote Imaging System (OSIRIS) on board of Rosetta [1] took 462 images covering more than 50% of Lutetia's surface with a maximum resolution of 60 m/px.

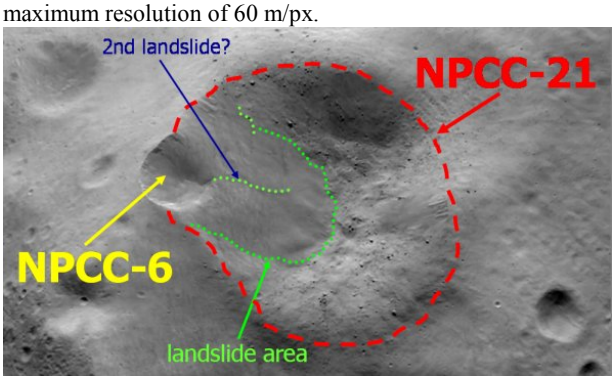

Fig. 1 Main features within the fresh 21 km crater NPCC-21.

Images from the North Pole Craters Cluster (NPCC) of the Baetica region show large topographical slope variations (from 0 to 45 degrees) and reveal evidence for major modification processes, such as landslides [2]. This region locates one of Lutetia's largest craters with a diameter of 21 [3] to 24 km [4], named NPCC-21 hereafter (see Fig. 1). The crater appears to be relatively young. Boulders sized up to 300 m are visible inside the cavity and along the rim [3,5]. The regolith layer is estimated up to several hundred meter in thickness [5-7] and at least one large landslide occurred at the crater rim [3]. A small 6-km-diameter structure (named NPCC-6 hereafter) is located at the rim of NPCC-21 that most likely originates from another impact [3]. The location of the crater at the top of the landslide area suggests that this impact event may have triggered the landslide. It is still uncertain, whether the asymmetric shape of NPCC-6 is due to topography or the landslide event. The example may serve as an excellent case study to investigate the effect of topography on crater formation, crater morphology and ejecta distribution. Three-dimensional (3D) numerical simulations are required to study such complex impact scenarios.

In this study, we present a suite of numerical models of crater formation on targets with topography and relate the results to the NPCC-6 impact event on the slope of the NPCC-21 crater.

Model setup: We used the three-dimensional, multi-material and multi-rheology hydrocode iSALE-3D [8,9] to model impacts into tilted targets (see Fig. 2) on Earth (gravity g=9.81 m/s^2) and Lutetia (g=0.05 m/s^2). We varied the projectile diameter L, the impact velocity U as well as the slope α_s and height ΔH of the hillside. We changed the impact direction by varying both impact angle α (measured from the horizontal) and striking angle α_v (measured from the vertical plane; see Fig. 2). The mechanical response of the material was modeled with a Drucker-Prager strength model where the yield strength $Y = Ycoh + f P$. We varied the coefficient of internal friction (f=0.2-0.7) and cohesion (Y_{coh}=0.1-1.8 MPa) to investigate the effect of strength.

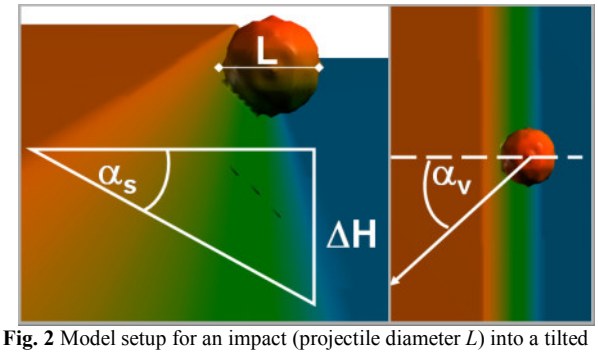

Fig. 2 Model setup for an impact (projectile diameter L) into a tilted target. Slope is defined by its angle α_s and height ΔH. Impact direction is defined by the impact angle α measured from the horizontal and a second angle α_v as shown in the right figure.

To model the NPCC-6 impact event, we used ANEOS tables [10] for dunite to compute the thermodynamic state of the material and assumed Y_{coh}=1 kPa and f=0.4. Local weakening is considered by acoustic fluidization [11] and porosity is neglected so far. We assumed a projectile diameter of L=1000 m, an impact velocity of U=4.2 km/s and varied the impact angle (α=20-45°; α_v=180-270°). The pre-landslide slope of the NPCC-21 crater rim is estimated to be 35°.

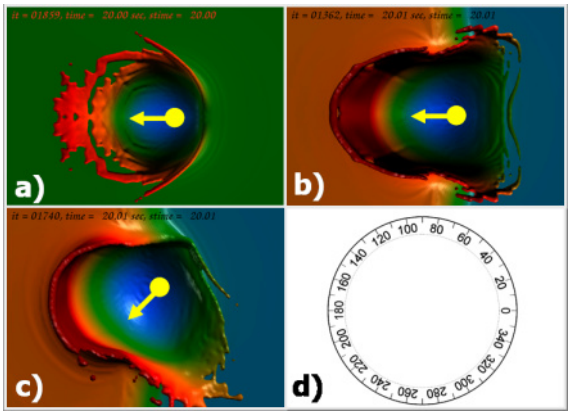

Fig. 3 Results for U=5 km/s, L=1 km, α=45°. a) Planar target; b) Impact perpendicular to titled targed (α_v=0°); c) oblique impact into tilted target (α_v=45°). d) Notation used for ejecta distribution presented in Fig. 4.

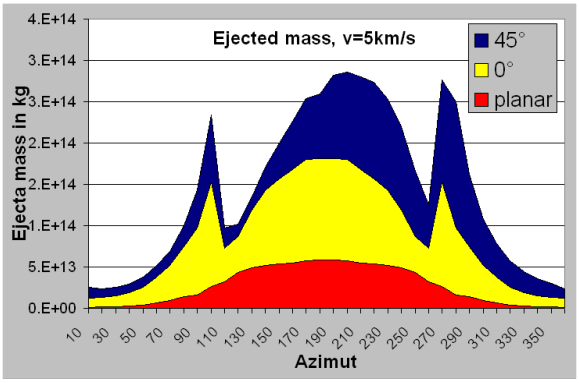

Fig. 4 Ejecta mass as a function of the azimuth (see Fig. 3d for definition).

Results: Figure 3 shows shapshots of an early stage of crater formation closely matching the *transient crater*. The images show an oblique (α=45°) impact (a) into a planar target, (b) striking a titled (45°) target vertically (α_v=0°), and (c) striking the same target at an oblique angle of incidence (α_v=45°). a) and b) result in a nearly circular crater shape whilst c) reveals an asymmetric cavity slightly elongated towards the lower level. The ejecta distribution of these three scenarios is compared in Fig. 4. Regardless of topography the maximum amount of ejecta in all cases is found downrange, which is 180° for a) and b), 225° for c). In these scenarios, topography increases the total amount of ejected material significantly. Deflected ejecta at the slope result in larger local accumulation of ejecta crossrange.

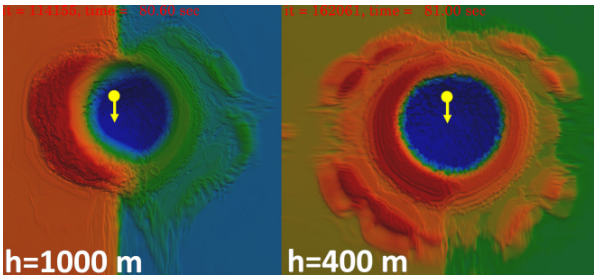

Fig. 5 Projectile (L=1400 m) striking a tilted (α_s=45°) target parallel to the slope (α_v=90°) at an angle of α=45° (velocity U=15 km/s). Comparison of the final craters for two different slope heights**.**

Fig. 5 shows a comparison of the effect of two different slope heights. We found that the crater shape is only influenced by impacts in tilted targets with a height of roughly 30% of the projectile's diameter or larger. Ejecta distribution is influenced by even lower differences in elevation, as clearly visible in Fig. 5.

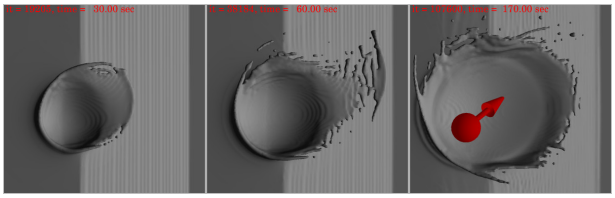

Fig. 6 Snapshots of the formation of NPCC-6 crater (here: impact angle α=45°, α_v=225°).

NPCC-6 formation. Since the depth of NPCC-21 (approx. 3 km [4]) is significantly larger than the projectile that formed NPCC-6 (we assumed L=1 km), it is very likely that the rim of NPPC-21 had an effect on the shape of NPCC-6. This is in good agreement with our preliminary results of the NPCC-6 formation based on 3D numerical modeling, shown in Fig. 6 and 7. We found (i) a derived crater structure of NPCC-6 that is in good agreement to observations by OSIRIS, (ii) a collapse of NPCC-6 which is strongly influenced by the rim of NPCC-21, (iii) indicators for an impact-triggered landslide.

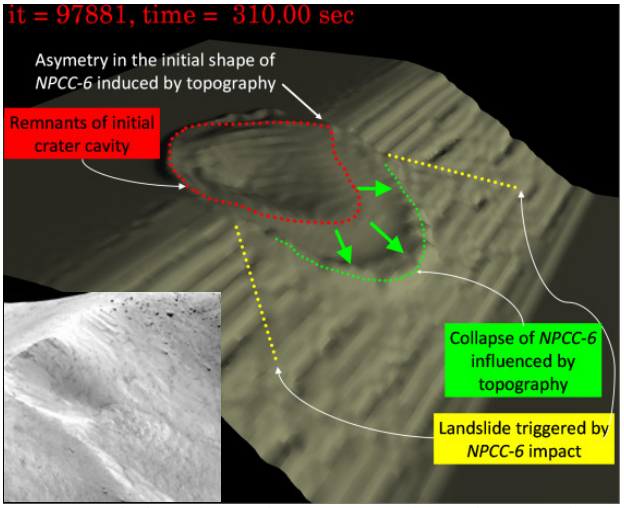

Fig. 7 Numerical simulation of NPCC-6 formation. Left: Perspective view of NPCC-6 (OSIRIS-image) for comparison.

Outlook: The results presented here are the first steps of a more detailed study of NPCC formation. Further tasks include (i) high resolution models of NPCC-6 formation, (ii) simulation of NPCC-21 formation to obtain better constraints for pre-landslide topography, (iii) simulation of NPCC-6 formation in a more complex geometry by using DTM data of NPCC-21, (iv) search for realistic impact conditions that allow triggering the landslide.

Acknowledgements: This work was funded by the Helmholtz-Alliance HA-203 / "Planetary Evolution and Life" by the Helmholtz-Gemeinschaft Deutscher Forschungszentren (HGF).

References: [1] Keller H. U. et al. (2007) *Space Sci. Rev. 128,* 433-506. [2] Marchi S. et al. (2011) *Planet. Space Sci.*, in press. [3] Thomas N. et al. (2011) *Planet. Space Sci.*, in press. [4] Cremonese G. et al. (2011) Planet. Space Sci., in press. [5] Küppers M. et al. (2012) *Planet. Space Sci.*, in press. [6] Vincent J. B. et al. (2011) *Planet. Space Sci.*, accepted. [7] Sierks H. et al. (2011) *Science 334*, 487-490. [8] Elbeshausen D. et al. (2009) *Icarus 204*, 716-731. [9] Elbeshausen D. and Wünnemann K. (2011) *Proc. HVIS XI*, 287-301. [10] Thompson S. L. and Lauson H. S. (1972) *Report SC-RR-71 0714,* Sandia National Lab., Albuquerque, New Mexico. [11] Wünnemann K. and Ivanov B.A. (2003). *Planet. Space Sci. 51*, 831-845.